

¹Poli Chandra REDDY, ¹Mummadisetty UMAMAHESWAR,
¹Singamala Harinath REDDY, ²Malaraju Chengal RAJU

ANALYSIS OF MHD NANOFLUID IN A ROTATING SYSTEM UNDER THE EXISTENCE OF HEAT ABSORPTION

¹Department of Mathematics, Annamacharya Institute of Technology and Sciences (Autonomous), Rajampet, INDIA
²Department of Mathematics, JNTUA College of Engineering, Pulivendula, A.P., INDIA

Abstract: An unsteady MHD free convective flow of nanofluids through porous medium bounded by a moving vertical semi-infinite permeable flat plate with constant heat sink in a rotating frame of reference is studied theoretically. The novelty is the consideration of constant heat sink and convective boundary condition in a rotating frame. The velocity along the plate i.e., slip velocity is assumed to oscillate in time with constant frequency so that the solutions of the boundary layer are the same oscillatory type. The dimensionless governing equations for this investigation are solved analytically using small perturbation approximation. The nanofluid namely TiO₂-water is taken into consideration. Heat and mass transfer characteristics under the influence of various physical parameters are discussed through graphs and tables. An increase in the convective parameter and nano particle volume fraction lead to increase the thermal boundary layer thickness but opposite effect occurs for heat absorption.

Keywords: Nanofluids, Convective boundary, heat and mass transfer, rotating system and porous medium

1. INTRODUCTION

Convective heat transfer in nanofluids is a major contemporary topic in sciences and engineering. Nowadays the development of high performance thermal systems for heat transfer enhancement has become popular. The enhancement of heating and cooling fluids in an industrial process saves energy, time and lifespan of the equipment. Heating and cooling fluids such as water, ethylene glycol and engine oil play a vital role in thermal management of high tech industries but they exhibit poor thermal characteristics in a certain thermal conductivity. To understand the heat transfer performance for the practical applications a number of works has been performed. Using nanofluid in a stretching surface Akbar et al. (2013) explained the radiation effects on MHD stagnation point flow with convective boundary condition. Bahiraei et al. (2017) gave assessment and optimization of hydrothermal characteristics for a non-Newtonian nanofluid flow within miniaturized concentric-tube heat exchanger considering designer's viewpoint. Bahiraei et al. (2018) analyzed development of chaotic advection in laminar flow of a non-Newtonian nanofluid: A novel application for efficient use of energy and Recent research contributions concerning use of nanofluids in heat exchangers: A critical review. Chamka et al. (2011) discussed MHD free convective flow past a vertical plate in the presence of heat generation or absorption effects using nanofluids. Chandra Reddy et al. (2018, 2019, 2020) examined MHD natural convective heat generating/ absorbing and radiating fluid past a vertical plate embedded in porous medium and derived an exact solution. Das (2014) discussed thoroughly flow and heat transfer characteristics of nanofluids in a rotating frame. Hamad et al. (2011) analyzed unsteady MHD free convective flow past a vertical permeable flat plate in a rotating system with constant heat source constant. Sheikholeslami et al. (2014) analyzed the three dimensional heat and mass transfer in a rotating system using nanofluid.

The objective of the present study is to analyze an unsteady MHD free convective flow of nanofluids through porous medium bounded by a moving vertical semi-infinite permeable flat plate with constant heat sink and convective boundary condition in a rotating frame. It is assumed that the plate is embedded in a uniform porous media and oscillates in time with constant frequency in the presence of transverse magnetic field.

2. MATHEMATICAL FORMULATION OF THE PROBLEM

Consider the unsteady three dimensional free convection flow of an electrically conducting incompressible nanofluid of ambient temperature T_∞ past a semi-infinite vertical permeable moving plate embedded in a uniform porous

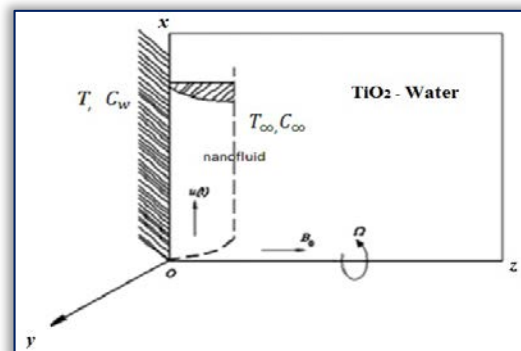


Figure 1: Physical model of the problem

medium embedded in a uniform porous

medium in the presence of thermal buoyancy effect with constant heat source and convective boundary condition. The fluid is a water based nanofluid containing TiO_2 nano particles. The nanoparticles are assumed to have a uniform shape and size. Moreover, it is assumed that both the fluid phase and nanoparticles are in thermal equilibrium state. The flow is assumed to be in x -direction which is taken along the plate in the upward direction and z -axis is normal to it. Also it is assumed that the whole system is rotated with a constant velocity Ω about z -axis as shown in Figure 1. A uniform external magnetic field B_0 is taken to be acting along the z -axis. It is assumed that there is no applied voltage which applies the absence of an electric field. Also it is assumed that the induced magnetic field is small compared to the external magnetic field. This implies a small magnetic Reynolds number for the oscillating plate. Due to semi-finite plate surface assumption, furthermore, the flow variables are functions of z and time t only.

Under the boundary layer approximations, the basic equations that describe the physical situation are given by

$$\frac{\partial w}{\partial z} = 0 \quad (1)$$

$$\frac{\partial u}{\partial t} + w \frac{\partial u}{\partial z} - 2\Omega v = \frac{1}{\rho_{nf}} \left[\frac{\partial^2 u}{\partial z^2} + (\rho\beta)_{nf} g(T - T_\infty) + (\rho\beta)_{nf} g(C - C_\infty) - \frac{\mu_{nf} u}{k} - \sigma B_0^2 u \right] \quad (2)$$

$$\frac{\partial v}{\partial t} + w \frac{\partial v}{\partial z} + 2\Omega u = \frac{1}{\rho_{nf}} \left[\mu_{nf} \frac{\partial^2 v}{\partial z^2} - \frac{\mu_{nf} v}{k} - \sigma B_0^2 v \right] \quad (3)$$

$$\frac{\partial T}{\partial t} + w \frac{\partial T}{\partial z} = \alpha_{nf} \frac{\partial^2 T}{\partial z^2} - \frac{Q}{(\rho C_p)_{nf}} (T - T_\infty) \quad (4)$$

$$\frac{\partial C}{\partial t} + w \frac{\partial C}{\partial z} = D \frac{\partial^2 C}{\partial z^2} \quad (5)$$

Further we assume that the plate surface temperature is maintained by convective heat transfer at a certain value which is to be determined later. Thus the boundary conditions are given by

$$u = v = 0, T = T_\infty \quad \text{for } t \leq 0 \quad (6)$$

$$u = U_r \left[1 + \frac{\varepsilon}{2} \{ \exp(int) + \exp(-int) \} \right], v = 0, C = C_w, -k_{nf} \frac{\partial T}{\partial z} = h_f T, \text{ at } z = 0$$

and $u \rightarrow 0, v \rightarrow 0, T \rightarrow T_\infty, C = C_\infty \quad \text{at } z \rightarrow \infty \quad (7)$

where U_r is the uniform reference velocity and ε is the small constant quantity. The oscillatory plate velocity assumed in equation (7) is based on the effective density of the nanofluid is given by

$$\rho_{nf} = (1 - \phi)\rho_f + \phi\rho_s \quad (8)$$

where ϕ is the solid volume fraction of nanoparticles.

Thermal diffusivity of the nanofluid is

$$\alpha_{nf} = \frac{k_{nf}}{(\rho C_p)_{nf}} \quad (9)$$

where the heat capacitance C_p of the nanofluid is obtained as

$$(\rho C_p)_{nf} = (1 - \phi)(\rho C_p)_f + \phi(\rho C_p)_s \quad (10)$$

and the thermal conductivity of the nanofluid k_{nf} for spherical nanoparticles can be written as

$$\frac{k_{nf}}{k_f} = \frac{(k_s + 2k_f) - 2\phi(k_f - k_s)}{(k_s + 2k_f) + \phi(k_f - k_s)} \quad (11)$$

The thermal expansion coefficient of the nanofluid can be determined by

$$(\rho\beta)_{nf} = (1 - \phi)(\rho\beta)_f + \phi(\rho\beta)_s \quad (12)$$

Also the effective dynamic viscosity of the nanofluid given by

$$\mu_{nf} = \frac{\mu_f}{(1 - \phi)^{2.5}} \quad (13)$$

where the subscripts nf, f and s represent the thermo physical properties of nanofluids, base fluid and nano solid particles respectively.

The continuity equation (1) gives

$$w = -w_0 \quad (14)$$

where the w_0 represents the normal velocity at the plate which is positive for suction and negative for injection.

Let us introduce the following dimensionless variables:

$$u' = \frac{u}{U_r}, v' = \frac{v}{U_r}, z' = \frac{zU_r}{v_f}, t' = \frac{tU_r^2}{v_f}, n' = \frac{nv_f}{U_r^2}, \theta = \frac{T - T_\infty}{T_\infty}, C' = \frac{c - c_\infty}{c_w - c_\infty} \quad (15)$$

Then substituting equations (15) into the equations (2)-(5) yields the following dimensionless equations (dropping primes)

$$\left[1 - \phi + \phi \left(\frac{\rho_s}{\rho_f} \right) \right] \left(\frac{\partial u}{\partial t} - S \frac{\partial u}{\partial z} - Rv \right) = \frac{1}{(1 - \phi)^{2.5}} \frac{\partial^2 u}{\partial z^2} + \left[1 - \phi + \phi \left(\frac{(\rho\beta)_s}{(\rho\beta)_f} \right) \right] (G_r \theta + G_c C) - \left(M^2 + \frac{1}{(1 - \phi)^{2.5} K} \right) u \quad (16)$$

$$\left[1 - \phi + \phi \left(\frac{\rho_s}{\rho_f} \right) \right] \left(\frac{\partial v}{\partial t} - S \frac{\partial v}{\partial z} + Ru \right) = \frac{1}{(1 - \phi)^{2.5}} \frac{\partial^2 v}{\partial z^2} - \left(M^2 + \frac{1}{(1 - \phi)^{2.5} K} \right) v \quad (17)$$

$$\frac{\partial C}{\partial t} - S \frac{\partial C}{\partial z} = \frac{1}{Sc} \frac{\partial^2 C}{\partial z^2} \quad (18)$$

$$\left[1 - \phi + \phi \left(\frac{(\rho C_p)_s}{(\rho C_p)_f} \right) \right] \left(\frac{\partial \theta}{\partial t} - S \frac{\partial \theta}{\partial z} \right) = \frac{1}{Pr} \left(\frac{k_{nf}}{k_f} \frac{\partial^2 \theta}{\partial z^2} - Q_H \theta \right) \quad (19)$$

Also the boundary conditions become

$$u = v = 0, \theta = 0 \quad \text{for } t \leq 0 \quad (20)$$

$$u = \left[1 + \frac{\varepsilon}{2} \{ \exp(int) + \exp(-int) \} \right], v = 0, \theta'(0) = -\gamma(1 + \theta(0)), C = 1 \quad \text{at } t = 0$$

and

$$v \rightarrow 0, \theta \rightarrow 0, C \rightarrow 0 \quad \text{as } z \rightarrow \infty \quad \text{for } t > 0 \quad (21)$$

We now simplify Eqs. (16) and (17) by putting the fluid velocity in the complex form as $V = u + iv$ then we get

$$\left[1 - \phi + \phi \left(\frac{\rho_s}{\rho_f} \right) \right] \left(\frac{\partial V}{\partial t} - S \frac{\partial V}{\partial z} - iRV \right) = \frac{1}{(1 - \phi)^{2.5}} \frac{\partial^2 V}{\partial z^2} + \left[1 - \phi + \phi \left(\frac{(\rho\beta)_s}{(\rho\beta)_f} \right) \right] (G_r \theta + G_c C) - \left(M^2 + \frac{1}{(1 - \phi)^{2.5} K} \right) V \quad (22)$$

The associated boundary conditions (20) and (21) are written as follows:

$$V = 0, \theta = 0 \quad \text{for } t \leq 0 \quad (23)$$

$$V(0) = \left[1 + \frac{\varepsilon}{2} \{ \exp(int) + \exp(-int) \} \right], \theta'(0) = -\gamma(1 + \theta(0))$$

$$V \rightarrow 0, \theta \rightarrow 0 \quad \text{as } z \rightarrow \infty \quad \text{for } t > 0 \quad (24)$$

where: $R = \frac{2\Omega v_f}{U_r^2}$ is the rotational parameter, $M = \frac{B_0}{U_r} \sqrt{\frac{\sigma v_f}{\rho_f}}$ is the magnetic field parameter,

$S = \frac{W_0}{U_r}$ is the suction ($S > 0$) or injection ($S < 0$) parameter, $Sc = \frac{v_f}{D}$ is the Schmidt number,

$K = \frac{kU_r}{v_f}$ is the permeability of the porous medium, $Q_H = \frac{Q v_f^2}{U_r^2 k_f}$ is the heat source parameter,

$G_r = \frac{v_f g \beta_f T_\infty}{U_r^3}$ is the Grashof number, $G_c = \frac{v_f g \beta_f (C_w - C_\infty)}{U_r^3}$ is the Solutal Grashof number, and

$\gamma = \frac{h_f v_f}{k_f U_r}$ is the convective parameter.

3. ANALYTICAL SOLUTIONS

To find the analytical solutions of the system of partial differentiation equations (18), (19) and (22) in the neighborhood of the plate under the boundary conditions (23), (24), we express V , C and θ as follows.

$$V(z, t) = V_0 + \frac{\varepsilon}{2} [\exp(int)V_1(z) + \exp(-int)V_2(z)] \quad (25)$$

$$C(z, t) = C_0 + \frac{\varepsilon}{2} [\exp(int)C_1(z) + \exp(-int)C_2(z)] \quad (26)$$

$$\theta(z, t) = \theta_0 + \frac{\varepsilon}{2} [\exp(int)\theta_1(z) + \exp(-int)\theta_2(z)] \quad (27)$$

Invoking the above Eqs. (25), (26) and (27) into (18), (19), (20) and equating the harmonic and non-harmonic terms and neglecting the higher order terms of ε^2 , we obtain the following set of equations.

$$\left[1 - \phi + \phi \left(\frac{\rho_s}{\rho_f} \right) \right] (-SV'_0 + iRV_0) = \frac{1}{(1-\phi)^{2.5}} V_0'' + \left[1 - \phi + \phi \left(\frac{(\rho\beta)_s}{(\rho\beta)_f} \right) \right] (G_r\theta + G_cC) - \left(M^2 + \frac{1}{(1-\phi)^{2.5}K} \right) V_0 \quad (28)$$

$$\left[1 - \phi + \phi \left(\frac{\rho_s}{\rho_f} \right) \right] (inV_1 - SV'_1 + iRV_1) = \frac{1}{(1-\phi)^{2.5}} V_1'' + \left[1 - \phi + \phi \left(\frac{(\rho\beta)_s}{(\rho\beta)_f} \right) \right] (G_r\theta + G_cC) - \left(M^2 + \frac{1}{(1-\phi)^{2.5}K} \right) V_1 \quad (29)$$

$$\left[1 - \phi + \phi \left(\frac{\rho_s}{\rho_f} \right) \right] (-inV_2 - SV'_2 + iRV_2) = \frac{1}{(1-\phi)^{2.5}} V_2'' + \left[1 - \phi + \phi \left(\frac{(\rho\beta)_s}{(\rho\beta)_f} \right) \right] (G_r\theta + G_cC) - \left(M^2 + \frac{1}{(1-\phi)^{2.5}K} \right) V_2 \quad (30)$$

$$\frac{1}{Sc} C_0'' + SC_0' = 0 \quad (31)$$

$$\frac{1}{Sc} C_1'' + SC_1' - inC_1 = 0 \quad (32)$$

$$\frac{1}{Sc} C_2'' + SC_2' + inC_2 = 0 \quad (33)$$

$$\frac{k_{nf}}{k_f} \theta_0'' + PrS \left[1 - \phi + \phi \left(\frac{(\rho C_p)_s}{(\rho C_p)_f} \right) \right] \theta_0' - Q_H \theta_0 = 0 \quad (34)$$

$$\frac{k_{nf}}{k_f} \theta_1'' + PrS \left[1 - \phi + \phi \left(\frac{(\rho C_p)_s}{(\rho C_p)_f} \right) \right] \theta_1' - \left(in Pr \left[1 - \phi + \phi \left(\frac{(\rho C_p)_s}{(\rho C_p)_f} \right) \right] + Q_H \right) \theta_1 = 0 \quad (35)$$

$$\frac{k_{nf}}{k_f} \theta_2'' + PrS \left[1 - \phi + \phi \left(\frac{(\rho C_p)_s}{(\rho C_p)_f} \right) \right] \theta_2' + \left(in Pr \left[1 - \phi + \phi \left(\frac{(\rho C_p)_s}{(\rho C_p)_f} \right) \right] + Q_H \right) \theta_2 = 0 \quad (36)$$

The corresponding boundary conditions can be written as

$$V_0 = V_1 = V_2 = 1, \theta_0' = \gamma(1 + \theta_0), \theta_1' = \gamma\theta_1, \theta_2' = \gamma\theta_2, C_0 = 1, C_1 = 0, C_2 = 0 \quad \text{at } z=0. \quad (37)$$

$$V_0 \rightarrow 0, V_1 \rightarrow 0, V_2 \rightarrow 0, \theta_0 \rightarrow 0, \theta_1 \rightarrow 0, \theta_2 \rightarrow 0, C_0 \rightarrow 0, C_1 \rightarrow 0, C_2 \rightarrow 0 \quad \text{as } z \rightarrow \infty \quad (38)$$

Solving the equations (28) to (36) under the boundary conditions (37) and (38) we obtain the expression for velocity, concentration and temperature as

$$V = (1 - A - B)e^{-m_{12}z} + Ae^{-m_2z} + Be^{-Scz} + \frac{\varepsilon}{2} (\exp(int)e^{-m_{10}z} + \exp(-int)e^{-m_s z}) \quad (39)$$

$$C = e^{-Scz} \quad (40)$$

$$\theta = \frac{\gamma}{m_2 - \gamma} e^{m_2 z} \quad (41)$$

where $m_2 = \frac{X_1 S + \sqrt{(X_1 S)^2 + 4XQ_H}}{2X}$; $X_1 = Pr \left[1 - \phi + \phi \left(\frac{(\rho C_p)_s}{(\rho C_p)_f} \right) \right]$; $X = \frac{(k_s + 2k_f) - 2\phi(k_f - k_s)}{(k_s + 2k_f) + \phi(k_f - k_s)}$; $\gamma = \frac{\lambda}{X}$;

$$m_{12} = \frac{Sk_1 + \sqrt{S^2 k_1^2 + 4(k_3 + ik_1)R}}{2}; m_{10} = \frac{k_1 S + \sqrt{k_1^2 S^2 + 4k_4}}{2}; A = \frac{-k_2 G_r \gamma}{(m_2 - \gamma)(m_2^2 - Sk_1 m_2 - (k_3 + ik_1)R)}$$

$$B = \frac{-k_2 G_c}{(Sc^2 - Sk_1 Sc - (k_3 + ik_1)R)}; k_1 = (1 - \phi)^{2.5} \left[1 - \phi + \phi \left(\frac{\rho_s}{\rho_f} \right) \right]; k_2 = (1 - \phi)^{2.5} \left[1 - \phi + \phi \left(\frac{(\rho\beta)_s}{(\rho\beta)_f} \right) \right]$$

$$k_3 = (1 - \phi)^{2.5} M^2 + \frac{1}{K}; k_4 = k_3 + ink_1 + ik_1 R; k_5 = k_3 + ink_1 - ik_1 R$$

4. RESULTS AND DISCUSSION

To analyze the properties of the flow the numerical results are presented in figures and tables. In the present study we have chosen $Pr = 7$, $n = 10$, $t = \pi/6$ and $\varepsilon = 0.02$. Figure 2 illustrates the influence of magnetic parameter M on velocity profile for the nanofluid TiO_2 -water. It shows that as the magnetic parameter M increases the velocity decreases across the boundary layer. The reason behind this nature is due to the retarding force by

the magnetic field which is known as Lorentz force. This force has the feature to slow down the motion of the fluid in the boundary layer. Figure 3 displays the fact that with the increase in rotational parameter R velocity decreases. Figure 4 demonstrates the velocity effect for various values of suction parameter ($S > 0$). It is clear that increase in suction parameter decreases the velocity across the boundary layer.

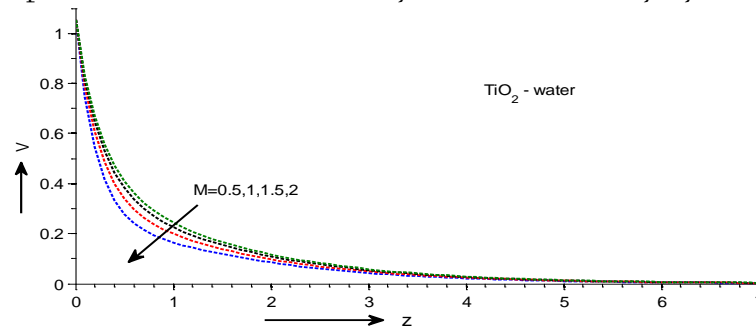


Figure 2: Velocity profiles for various values of M when $\gamma = 0.1$, $S = 0.5$, $Q_H = 5$, $R = 0.3$, $K = 0.1$, $Gr = 5$, $Gc = 5$.

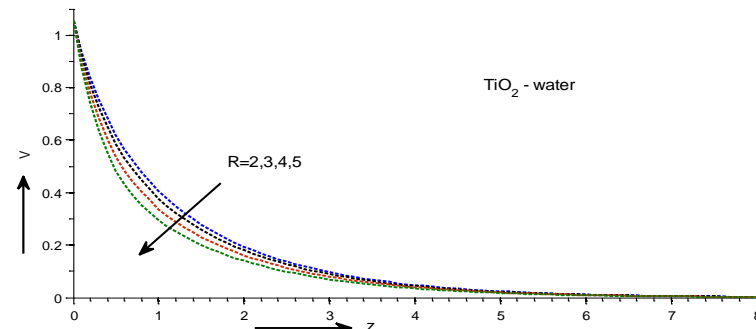


Figure 3: Velocity profiles for various values of R when $\gamma = 0.1$, $S = 0.5$, $Q_H = 5$, $M = 1$, $K = 0.1$, $Gr = 5$, $Gc = 5$.

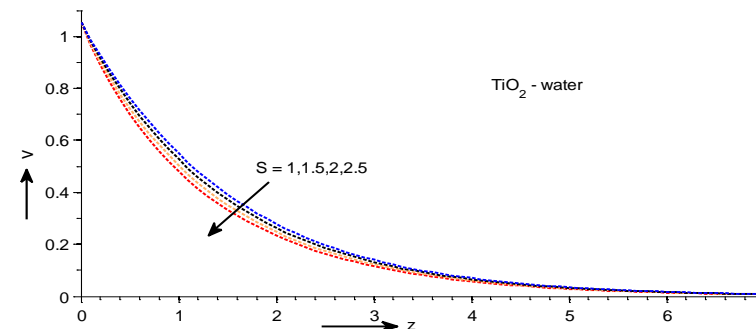


Figure 4: Velocity profiles for various values of S when $\gamma = 0.1$, $R = 0.3$, $Q_H = 5$, $M = 1$, $K = 0.1$, $Gr = 5$, $Gc = 5$.

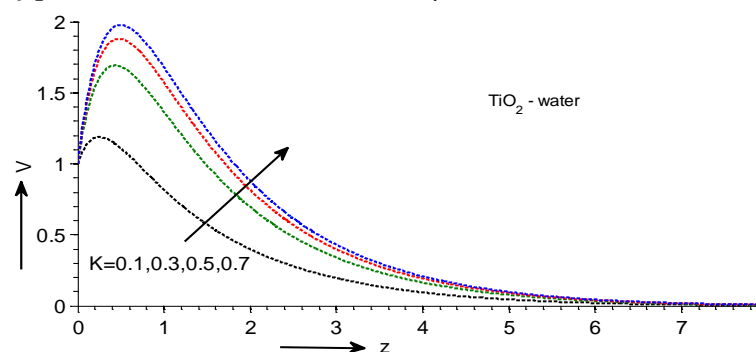


Figure 5: Velocity profiles for various values of K when $\gamma = 0.1$, $R = 0.3$, $S = 1$, $Q_H = 5$, $M = 1$, $K = 0.1$, $Gr = 5$, $Gc = 5$.

Figure 5 illustrates the velocity effects for different values of permeability parameter K on the porous medium. It is seen that the increase in permeability parameter leads to increase in velocity and improve the boundary layer thickness. This is due to the natural fact that the increase in porosity leads to free motion of the fluid and hence the velocity accelerates. Figures 6 & 7 display the velocity profiles for various values of Grashof number Gr and Solutal Grashof number Gc . The velocity increases with the increase in Gr and Gc across the boundary layer. The physical reason behind this is that mass transfer creates free movement in the fluid particles and so the fluid velocity enhances. Figure 8 exhibits the variation in velocity for different values of nano particle volume fraction parameter. It is clear that the velocity across the boundary layer decreases with the increase in nano particle volume fraction parameter. Figure 9 represents the changes in the distribution of

temperature for various values of convective parameter. It is found that the temperature rises for the enhancing values of convective parameter. Hence it tends to thermal boundary layer thickness enhancement. Figure 10 depicts the temperature profiles for various values of the heat source parameter Q_H . It reveals that for the increasing values of heat source parameter the temperature in boundary layer region decreases. Figure 11 presents the variations in the temperature distribution for different values of suction ($S > 0$) parameter. It is clear that increase in suction parameter decreases the temperature across the boundary layer.

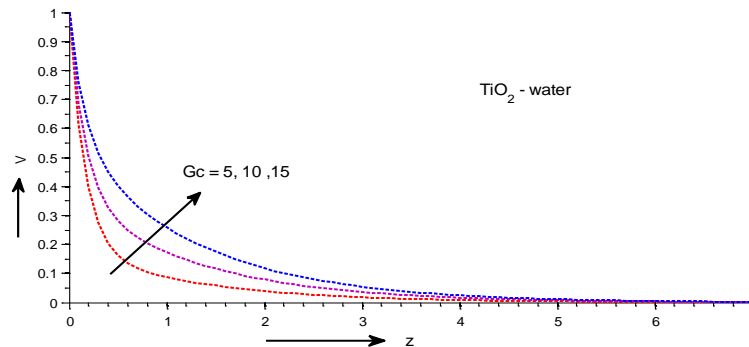


Figure 6: Velocity profiles for various values of G_c when $\gamma = 0.1, R = 0.3, K = 0.1, Q_H = 5, S = 1, M = 5, Gr = 5$.

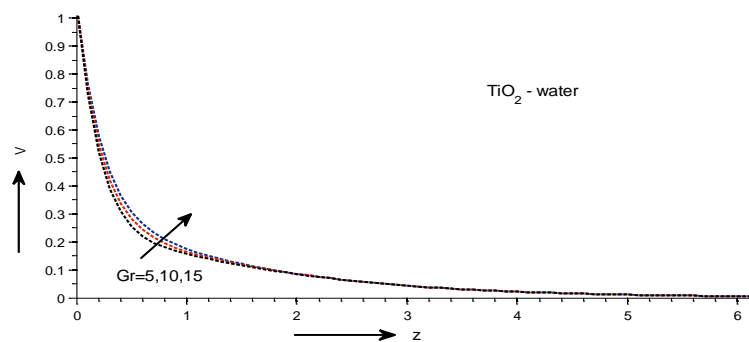


Figure 7: Velocity profiles for various values of Gr when $\gamma = 0.1, R = 0.3, K = 0.1, Q_H = 5, S = 0.1, M = 5, G_c = 5$.

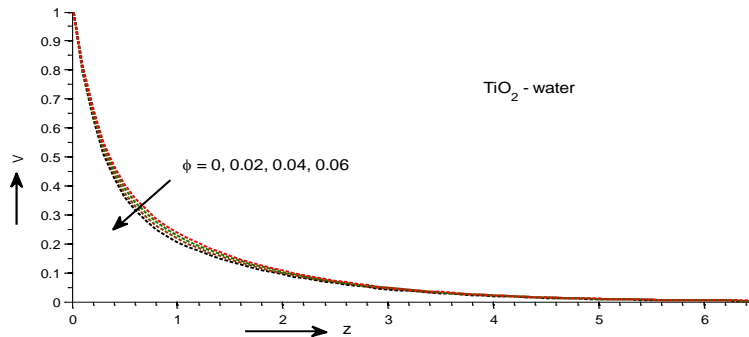


Figure 8: Velocity profiles for various values of ϕ when $R = 0.3, K = 0.1, Q_H = 5, S = 1, M = 1, Gr = 5, G_c = 5$.

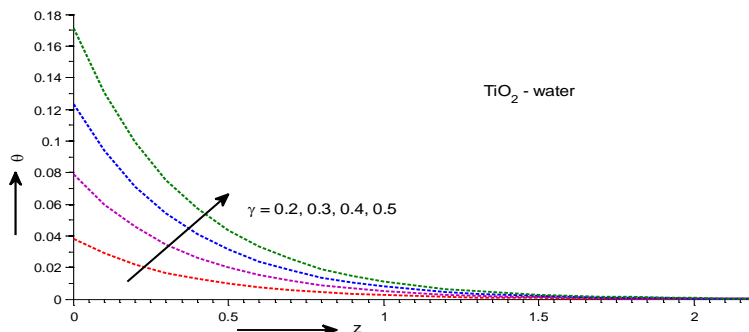


Figure 9: Temperature profiles for various values of γ when $R = 0.3, K = 0.1, Q_H = 5, S = 0.1, M = 1, Gr = 5, G_c = 5$.

Figure 12 shows the variations in concentration under the influence of Schmidt parameter. It can be observed that concentration over the fluid decreases for increasing values of Schmidt parameter. Thus the concentration field becomes thinner as it relates to the comparative thickness of hydrodynamic thickness and mass transfer. Figure 13 reveals that for the increasing values of the volume fraction parameter temperature profiles increases.

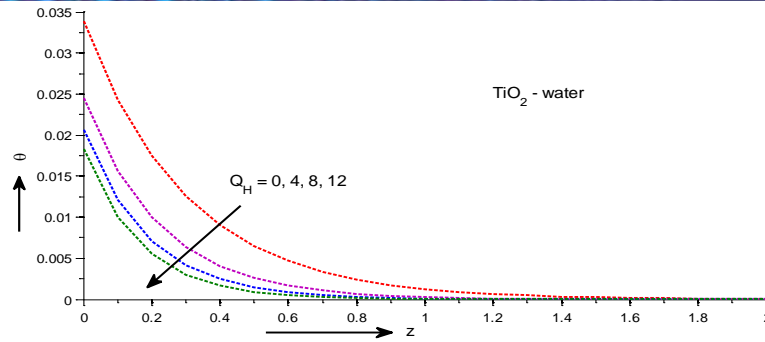


Figure 10: Temperature profiles for various values of Q_H when $R= 0.3, K=0.1, \gamma=0.1, S=0.1, M=1, Gr = 5, Gc=5$

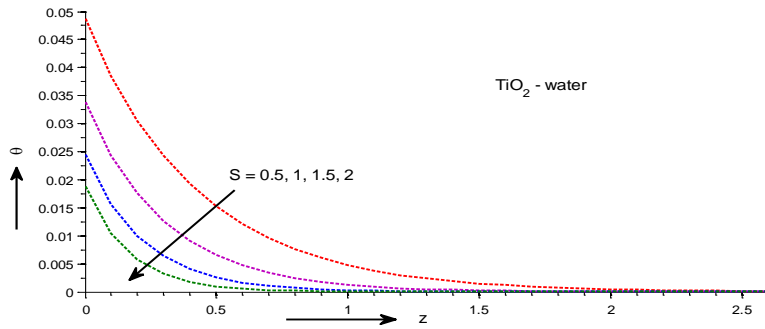


Figure 11: Temperature profiles for various values of S when $R= 0.3, K=0.1, \gamma=0.1, Q_H=5, M=1, Gr = 5, Gc=5$

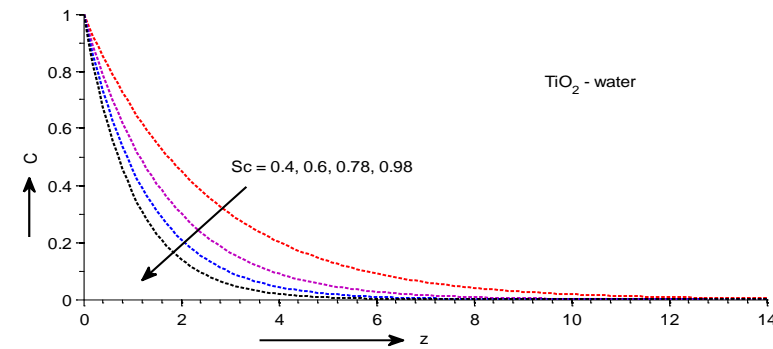


Figure 12: Concentration profiles for various values of Sc when $R= 0.3, K=0.1, \gamma=0.1, Q_H=5, M=1, Gr = 5, Gc =5$

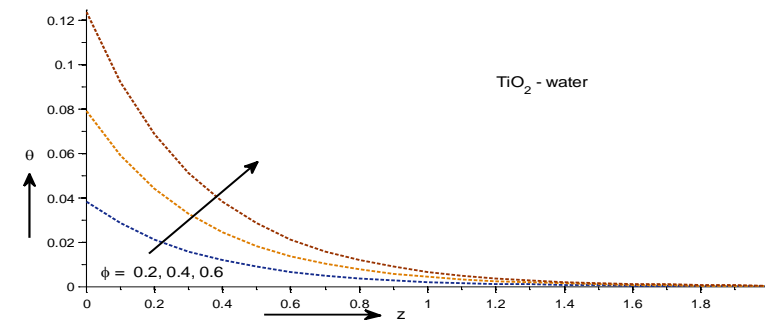


Figure 13: Temperature profiles for various values of ϕ when $R= 0.3, K=0.1, \gamma=0.1, Q_H=5, M=1, Gr = 5, Gc=5$

Table 1 represents the thermo physical properties of regular fluid and nanoparticles. Table 2 shows the effect of magnetic parameter, convective parameter and Schmidt number on skin friction coefficient, Nusselt number and Sherwood number. It shows that as the magnetic parameter M increases skin friction coefficient increases with specific permeability parameter, Prandtl number and Schmidt number. Skin friction coefficient decreases with an increase in the convective parameter and Nusselt number increases with the increase in convective parameter. But no change is seen in Sherwood number. It is observed the both skin friction coefficient and sherwood number increases for the increasing values of the schmidt

Table 1: Thermo physical properties of regular fluid and nanoparticles.

Physical properties	Water/base fluid	TiO ₂ (Titanium Oxide)
ρ (kg/m^3)	997.1	4250
C_p ($J/kg K$)	4179	686.2
k ($W/m K$)	0.613	8.9538
$\beta \times 10^5$ (K^{-1})	21	0.90
ϕ	0.0	0.2
σ (S/m)	5.5×10^{-6}	2.6×10^6

parameter but there is no change in Nusselt number. From Table 3, we observe that the skin friction coefficient at the plate decreases with an increase in rotational parameter. But there is no change in Nusselt number and Sherwood number. An increase in the permeability parameter tends to decrease in the skin friction coefficient but there is no significant effect on Nusselt number. Table 3 shows the variations of heat source parameter on skin friction coefficient, Nusselt number and Sherwood number. It is noticed that both skin friction coefficient and Nusselt number increases with the increase in heat source parameter.

Table 2: Values of τ, Nu, Sh for different values of nanoparticles of M, γ, Sc

M	γ	Sc	TiO ₂ - Water		
			τ	Nu	Sh
0	0.1		2.4397	0.0101	0.078
0.5			2.4999		
1			2.6729		
1.5			2.9395		
2			3.2773		
1	0.1		2.6729	0.0101	
	0.2		2.667	0.0205	
	0.3		2.6613	0.0311	
	0.4		2.6554	0.042	
	0.5		2.6492	0.0532	
	0.1	0.22	2.3571	0.0101	0.022
		0.4	2.4719		0.04
		0.6	2.5841		0.06
		0.78	2.6777		0.078
		0.98	2.7598		0.098

Table 3: Values of τ, Nu, Sh for different values of nanoparticles of R, K, Q_H.

R	K	Q _H	TiO ₂ - Water	
			τ	Nu
0.3	0.1	5	2.4381	0.0104
		10	2.3732	0.0103
		15	2.3648	0.0102
		20	2.3631	0.0102
0.1	0.1	5	2.4381	0.0104
	0.2		0.5588	
	0.3		0.3904	
0.1	0.1		2.4246	
0.2			2.4290	
0.3			2.4381	
0.4			0.7146	

5. CONCLUSIONS

The main conclusions emerging from this study are as follows:

- In boundary layer region, the fluid velocity decreases with the increase in magnetic parameter, suction parameter, nano particle volume fraction and rotational parameter but effect is reverse in the case of permeability parameter.
- An increase in the convective parameter and nano particle volume fraction lead to increase the thermal boundary layer thickness but opposite effect occurs for heat absorption.
- In boundary layer region, the fluid concentration decreases with increasing values of Schmidt number.
- Skin friction coefficient as well as Nusselt number decreases under the influence of heat absorption.

References:

- [1] Akbar, N.S; Nadeem, S; Ul Haq, R and Khan, Z.H: Radiation effects on MHD stagnation point flow of nanofluid towards a stretching surface with convective boundary condition, Chin. J. Aeronaut., 26(6), 1389–1397, 2013.
- [2] Bahiraei, M; Khosravi, R and Heshmatian, S: Assessment and optimization of hydrothermal characteristics for a non-Newtonian nanofluid flow within miniaturized concentric-tube heat exchanger considering designer's viewpoint, Applied Thermal Engineering, 123, 266–276, 2017.
- [3] Bahiraei, M; Rahmani, R; Yaghoobi, A; Khodabandeh, E; Mashayekhi, R and Amani, M: Recent research contributions concerning use of nanofluids in heat exchangers: A critical review, Applied Thermal Engineering, 133, 137–159, 2018.
- [4] Chamka, A.J. and Aly, A.M: MHD free convective flow of a nanofluid past a vertical plate in the presence of heat generation or absorption effects, Chem. Eng. Comm., 198, 425–441, 2011.
- [5] Chandra Reddy, P; Harinath Reddy, S; Sivaiah, G; Ravi Kumar, V and Raju, M.C: Three dimensional laminar flow of magnetite water based nanofluids under heat generation and couple stress effects, JP Journal of Heat and Mass Transfer, 19(1), 19–29, 2020.
- [6] Chandra Reddy, P; Raju, M.C. and Raju, G.S.S: MHD natural convective heat generating/ absorbing and radiating fluid past a vertical plate embedded in porous medium—an exact solution, Journal of the Serbian Society for Computational Mechanics, 12(2), 106–127, 2018.
- [7] Chandra Reddy, P; Venkateswara Raju, K; Umamaheswar, M and Raju, M.C: Buoyancy effects on chemically reactive magneto-nanofluid past a moving vertical plate, Bulletin of Pure and Applied Sciences, 38E (1), 193–207, 2019.
- [8] Das, K: Flow and heat transfer characteristics of nanofluids in a rotating frame, Alexandria Engineering Journal, 53, 757–766, 2014.
- [9] Hamad, M.A.A. and Pop, I: Unsteady MHD free convective flow past a vertical permeable flat plate in a rotating frame of reference with constant heat source in a nanofluid, Heat Mass Transf., 7, 1517–1524, 2011.
- [10] Rehman, K.U; Malik, A.A; Malik, M.Y. and Zehra, M.T.I: On new scaling group of transformation for Prandtl-Eyring fluid model with both heat and mass transfer, Results in Physics, 8, 552–558, 2018.
- [11] Sheikholeslami, M and Ganji, D.D: Three dimensional heat and mass transfer in a rotating system using nanofluid, Power Techno., 253, 789–796, 2014.

copyright © University POLITEHNICA Timisoara, Faculty of Engineering Hunedoara,
5, Revolutiei, 331128, Hunedoara, ROMANIA

<http://annals.fih.upt.ro>